Effect of welding defects on plastic behaviour and fatigue lifetime of friction stir welded Al-Cu-Li alloy

Thomas Le Jolu, Thilo F. Morgeneyer, Anne Denquin, Anne-Françoise Gourgues-Lorenzon

Effect of welding defects on plastic behaviour and fatigue lifetime of friction stir welded Al-Cu-Li alloy

Thomas Le Jolu[1,2], Thilo F. Morgeneyer[1,*], Anne Denquin[3], Anne-Françoise Gourgues-Lorenzon[1]

[1] MINES ParisTech, Centre des Matériaux, UMR CNRS 7633, BP 87, 91003 Evry cedex, France
[2] Now at CEA Saclay, 91191 Gif-sur-Yvette cedex, France
[3] Onera BP 72-29 Avenue de la Division Leclerc 92322 CHATILLON cedex, France
* Corresponding author: thilo.morgeneyer@mines-paristech.fr

Abstract The effects of joint line remnant (JLR), kissing bond (KB), and clearance between the sheets (Gap) on tensile and fatigue properties of 2198-T851 friction stir welds have been quantitatively evaluated with respect to a reference weld made using one single sheet. The JLR has no significant influence in the investigated conditions. KB and Gap-induced defects do not significantly influence plastic yield but may induce premature crack initiation by ductile tearing and intergranular decohesions respectively. A critical value for KB opening (280 MPa), a threshold value for fatigue crack propagation from the KB (1 MPa√m) and crack growth rates consistent with literature data have been determined.

Keywords Friction stir welds, Welding defects, Tensile properties, Fatigue resistance

1. Introduction

Friction stir welding (FSW) of so-called “non-weldable” Al-Cu alloys has been developed to substitute riveting in lightweight structures [1]. It allows avoiding hot cracking and limiting component distortion. Internal flaws that are difficult to detect by using non-destructive evaluation (NDE) may appear under certain processing conditions. After welding, the natural oxide layer at butt surfaces may yield a defect [2-6] sometimes called “joint line remnant” (JLR). If the JLR is connected to the weld root and induces fracture after severe bending of the weld (e.g. [3, 7-8]), it is often referred to as a “kissing bond” (KB). In butt-welding conditions, a “Gap” might be left between the two sheets, leading to poor mixing of matter during FSW. The impact of such defects on tensile and fatigue properties has only been scarcely investigated [9-10]. The purpose of the present study is to compare the effects of JLR, KB and Gap-induced features on the tensile behaviour and fatigue lifetime of FSW joints of an Al-Cu-Li alloy dedicated to aircraft applications.

2. Experimental details

2.1. Materials and welding conditions

A 3.1-mm-thick sheet of AA2198-T851 with chemical composition Al-3.20 Cu - 0.98 Li - 0.31 Ag - 0.31 Mg - 0.11 Zr - 0.04 Fe - 0.03 Si (wt %) was considered. The sheet had been aged at 155°C for 16h. Pancake-shaped grains (10 - 20 µm in thickness) were observed in this material (Fig. 1). The hardness of this material was around 150±5 $HV_{0.1}$, except at mid-thickness (137±5 $HV_{0.1}$).

FSW butt joints were realised along the rolling direction using 500 mm (RD) x 150 mm (TD) coupons. Optimised welding parameters allowed minimising external defects such as flashes. Except for Gap bearing welds, the welding machine was displacement-controlled with a travelling speed of 480 $mm.min^{-1}$, a rotational speed of 1200 rpm, a conventional retractable tool with 13 mm in shoulder diameter and 4.2 mm in pin diameter. “Sound” welds were made by moving the tool into a single sheet, to avoid any native oxides at edges before welding. “JLR bearing” welds resulted from natural oxidation of the coupons before welding. “KB bearing” welds were fabricated

as for JLR but with retracting the pin by 80 µm to modify mixing conditions within the weld. "Gap bearing" welds were realised under load control with a constant clearance between the sheets, of either 0.3 mm ("Gap3": 10% of the parent sheet thickness) or 0.7 mm ("Gap7": 23% of the parent sheet thickness). Only KB bearing welds cracked under severe bending conditions (width 10 mm, bending angle 90°, bending radius 7 mm, and bottom part of the weld outside).

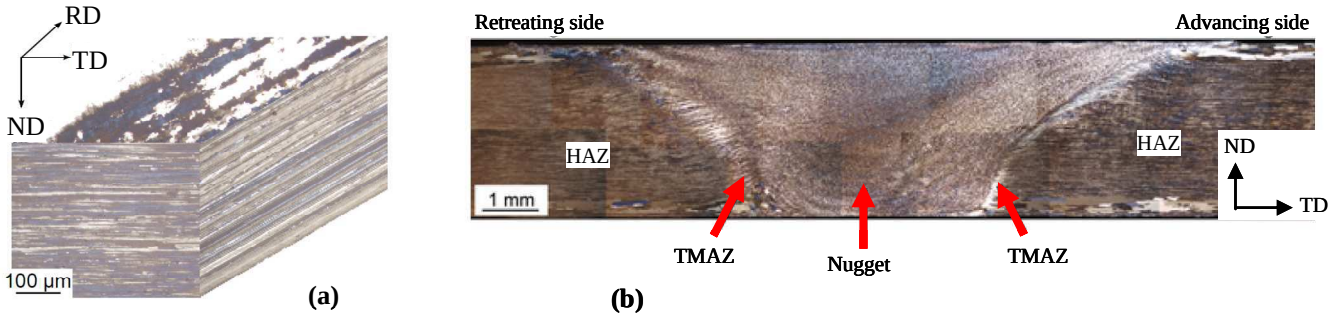

Figure 1. General view (a) of the grain structure of the studied sheet and (b) of a FSW joint (TMAZ: thermo-mechanically affected zone; HAZ: heat-affected zone)

The JLR appears as a dark line across the nugget (Fig. 2a). The KB has the same appearance as the JLR (Fig. 2b). Detailed observations revealed that this defect is intergranular [11]. In the Gap bearing samples, small regions with deeply etched grain boundaries ("sensitive GBs" hereafter) were observed from place to place in the nugget, at the bottom surface (Fig. 2c). The hardness profile (Fig. 3a) is identical for all welds. A minimum in hardness was detected at TMAZs, as already reported e.g. in a 2098-T8 friction stir weld [12].

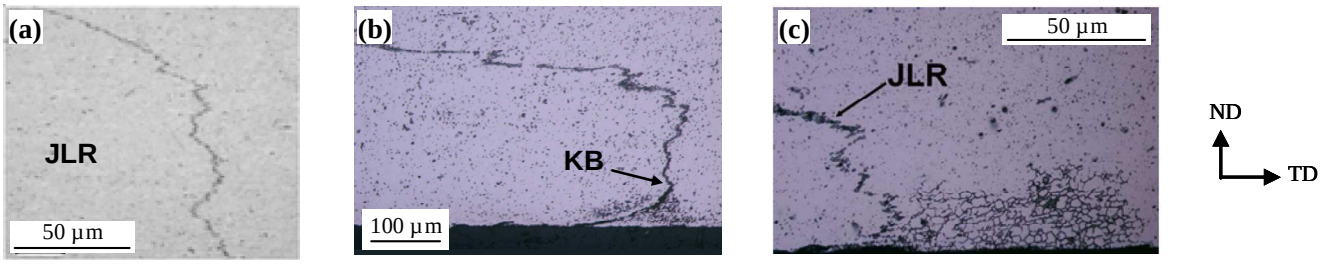

Figure 2. Cross-section observations of weld defects: (a) JLR; (b) KB (bottom) and JLR (upper, nearly horizontal part); (c) etched grain boundaries (bottom) and JLR in a Gap3 bearing weld

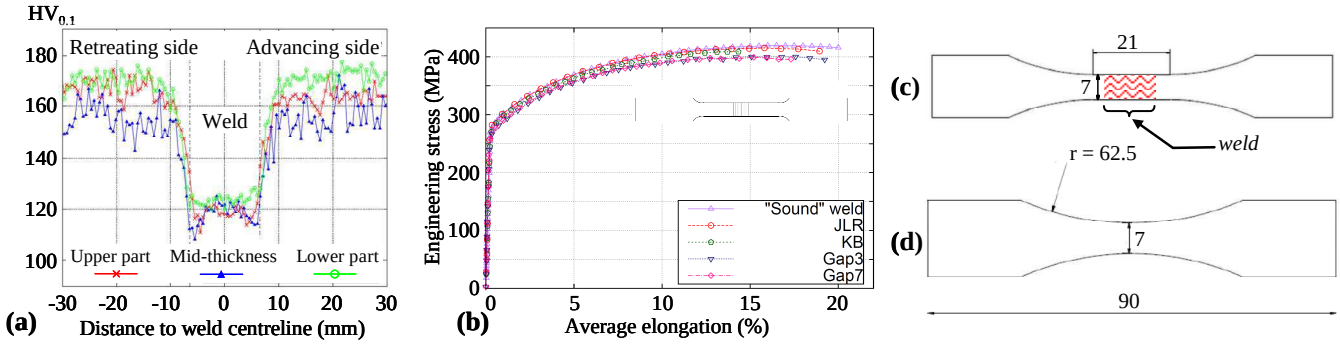

Figure 3. (a) Hardness profiles across a sound weld. (b) Tensile curves of the various kinds of welds. Drawings of full-thickness (c) cross-weld and (d) base metal fatigue specimens (dimensions in mm)

2.2. Mechanical testing

2.2.1. Uniaxial tensile tests

At least two full-thickness smooth tensile specimens (64x12 mm² in gauge dimensions) were cut across each welded joint and pulled in tension, in room temperature laboratory air, using a 250 kN servohydraulic testing machine under displacement control (elongation rate: 2.10^{-4} s^{-1} based on a gauge length of 14 mm). Local strains were monitored thanks to a random black-and-white speckle deposited onto the specimen and to conventional strain field monitoring techniques. Incremental calculation of displacements and strains was selected. To determine the onset of KB opening, an in situ tensile test on a miniature dogbone specimen (full thickness, 3×13 mm² in gauge dimensions) was carried out in the SEM, while observing the slightly polished bottom surface of the nugget.

2.2.2. Uniaxial fatigue tests

Uniaxial fatigue tests were performed on full-thickness specimens along TD (Fig. 3c,d). A straight gauge part was chosen for the cross-weld specimen, in order to study the fatigue crack initiation site under a homogeneous nominal stress (i.e., load divided by the initial area of the bearing section). All specimen corners and edges were slightly ground using 1200-grit SiC paper, except otherwise stated, to limit the influence of surface irregularities on fatigue crack initiation. Fatigue specimens were tested in room temperature laboratory air, under load control, with a load ratio of 0.1 and a frequency of 20 Hz. Most of the tests were carried out up to fracture.

A few tests were started at a lower frequency (0.5 Hz) for the first 10 cycles together with strain field monitoring on one edge thanks to the digital image correlation as described previously. Then, the frequency was changed to 20Hz. After a given fraction of the estimated lifetime at that load level, these tests were interrupted and the specimens were fractured under uniaxial tension.

2.3. Microstructural observations

Metallographic samples were polished in cross-section with diamond paste and first etched by anodic oxidation (3% aqueous solution of tetrafluoroboric acid in water, under 30 V with respect to pure Al, for 2-3 min) and then further chemically etched with the Dix-Keller reagent (2 mL HF, 3 mL HCl, 20 mL HNO_3, and 175 mL distilled water) and observed using optical microscopy under white light. Fracture surfaces were observed using a Leo 1540VP or a Zeiss DSM 982 Gemini scanning electron microscope (SEM) in secondary electron imaging. After each test, one specimen half was cut along the TD-ND plane at the crack initiation site, polished and etched using the above procedure to determine the influence of welding defects on crack initiation and propagation.

3. Experimental results and discussion

3.1. Tensile properties

No significant effect of the welding conditions was detected on tensile properties of JLR and KB bearing welds, with respect to sound welds (Fig. 3b). The yield strength and tensile strength of the welds were lower than those of the base metal (along the same loading direction) by about 40 and 20%, respectively (Table 1). Strain field measurements yielded identical results for all welds, except for a slight strain localisation at the bottom surface of the Gap7 bearing nugget [11].

All cross-weld specimens failed by strain localization, followed by ductile fracture. Sound welds fractured from close to the TMAZ-HAZ boundary with mixed dimpled / "fibrous" fracture surfaces (Fig. 4a). No obvious effect of the JLR was evidenced, as already reported by [1, 5, 13-14].

Table 1. Yield strength, tensile strength and ratio of weld tensile strength to that of base metal (along TD)

Weld	Yield strength (MPa)	Tensile strength (MPa)	Ratio of weld strength to base metal strength
Sound	282-302	412-429	0.80-0.83
JLR bearing	285-296	413-416	0.80
KB bearing	265-287	398-410	0.77-0.80
Gap3 bearing	282-284	401-404	0.78
Gap7 bearing	277-281	398-399	0.77

In KB bearing specimens, fracture initiated as a striated, locally ductile region whose location and geometry closely matched those of the KB itself (Fig. 4b), as in [7]. The crack then left the KB to propagate across the nugget. From in situ tensile tests, opening of the KB (Fig. 4c) occurred for an engineering stress higher than about 280 MPa (more details are reported in [11]). Multiple crack initiation sites were found in that case.

No effect of "sensitive GBs" was detected for the Gap3 bearing welds, whereas intergranular cracking triggered fracture of Gap7 welds (Fig. 4d). As already reported in [9], a clearance of 10% of the parent sheet thickness may be high enough to induce a decrease in strength. A clearance of 23% of the parent sheet thickness is high enough, in the investigated conditions, to trigger intergranular crack initiation and propagation from the nugget root.

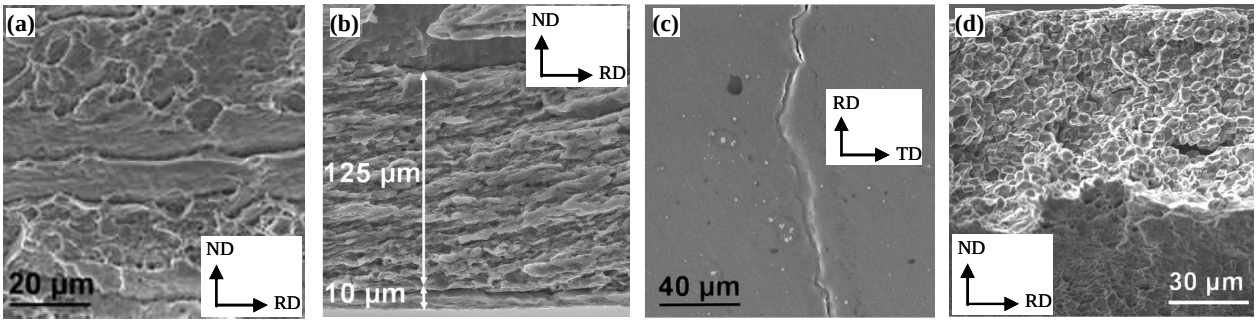

Figure 4. (a,b,d) fracture surfaces (a) in the TMAZ (sound and JLR bearing welds), (b) of a KB bearing weld (the striated zone corresponding to the KB defect itself) and (d) close to the root of a Gap7 weld. (c) Onset of cracking at the lower surface of a KB bearing specimen, slightly polished and then pulled in tension in the SEM (loading axis horizontal)

3.2. Fatigue properties

Fatigue properties of base metal and welds are summarized in Fig. 5 and Table 2. Despite of the high experimental scatter, the cross-weld specimens can be ranged as follows, with respect to their fatigue strength (Fig. 5 and Table 2):

Sound > JLR bearing > KB bearing (as-welded) > KB bearing (ground) > Gap3, Gap7 (1)

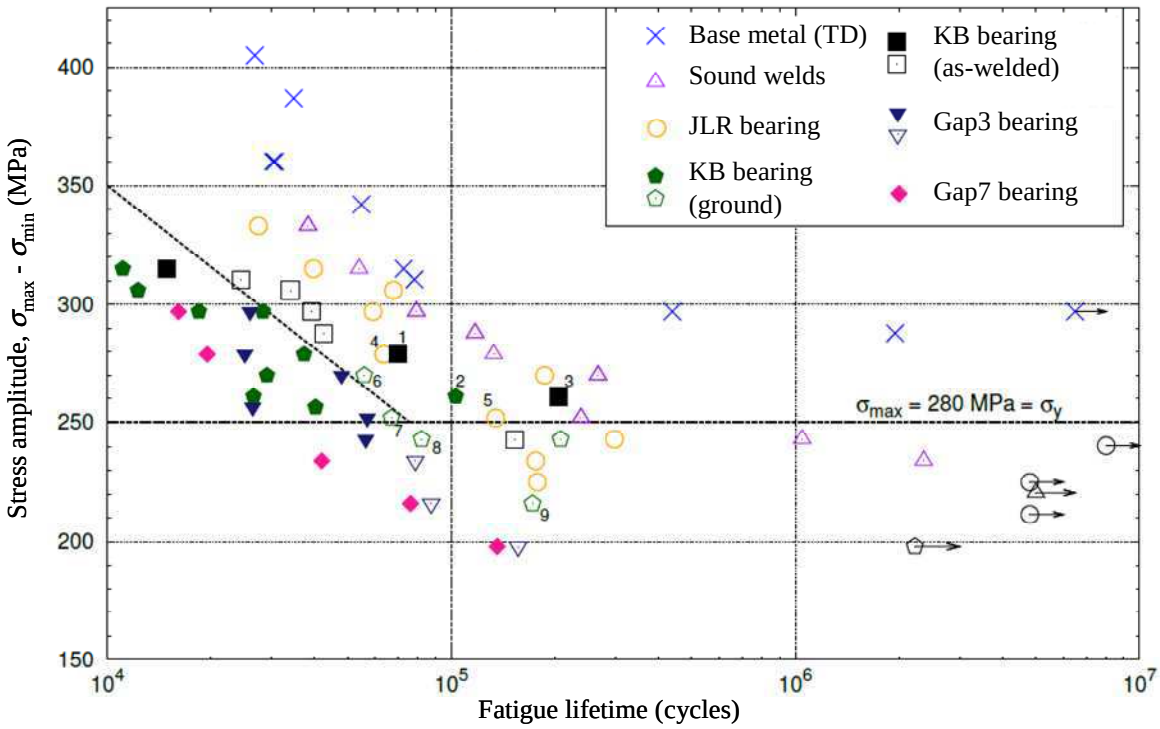

Figure 5. Fatigue lifetime of base metal, sound and defect bearing welds. Full symbols indicate that fracture initiated from the investigated weld defect. For all tests above the horizontal line, large scale yielding occurred during the first cycle. Comments on the numbered symbols: see text

Table 2. Fatigue strength, estimates of the number of cycles at crack initiation and crack initiation sites

Specimens	$\Delta\sigma$ at 10^5 cycles (MPa)	Relative difference with respect to sound welds (%)	Number of cycles at crack initiation (ratio to lifetime)	Crack initiation locus (number of specimens)
Base metal (TD)	315	+7%	-	-
Sound welds	280	-	> 50%	nugget (3) TMAZ / HAZ (6)
JLR bearing welds	270	-7%	≈ 50%	nugget far from JLR (6) HAZ (4)
KB bearing welds, ground	240	-17%	≈ 0 (0.25 cycle)	nugget far from KB (1) HAZ (4) KB (9)
KB bearing welds, as-welded	270	-7%	≈ 0 (0.25 cycle)	nugget far from KB (2) TMAZ/HAZ (3) KB (3)
Gap3 bearing welds, as-welded	210	-28%	≈ 0 (0.25 cycle)?	HAZ (3) sensitized GBs (6)
Gap7 bearing welds, as-welded	210	-28%	≈ 0 (0.25 cycle)?	sensitized GBs (5)

3.2.1. Fatigue properties of sound welds

The fatigue lifetime of sound welds is close to that of the base metal for higher loads, despite of their lower strength. From strain field monitoring, plastic yielding occurred during the first cycle and from the second cycle, only elastic strains were detected. The loss in fatigue strength (about 10%) of sound welds with respect to base metal, for lifetimes higher than ~10^5 cycles is lower than that reported by Cavaliere et al. [15] for a load ratio of 0.33 and a lifetime of 3.10^5 cycles (about 22%). This might be due to the difference in specimen surface preparation (Cavaliere et al. used polished surfaces) or in welding parameters.

Fatigue cracks in sound welds initiated either at the TMAZ/HAZ or within the nugget. Typical fracture surfaces observed in the nugget are shown in Fig. 6. Typical striations are observed in the Stage II crack propagation regime. No fatigue crack was detected either in the fracture surface or in a longitudinal cross-section after interrupted testing ($\Delta\sigma$ = 270 MPa, test interrupted after 50,000 cycles ~ 50% of fatigue lifetime). Consequently, the lifetime at crack initiation was higher than 50% of total lifetime in the considered case.

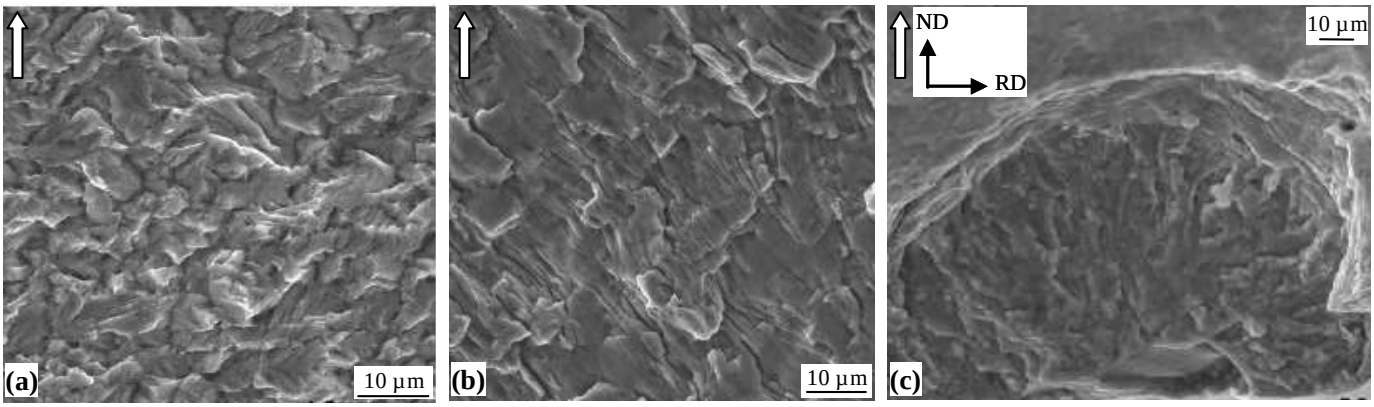

Figure 6. (a,b) Fracture surface of a sound weld ($\Delta\sigma$ = 270 MPa, lifetime ~ 133,000 cycles): (a) onset of crack propagation in the nugget; (b) Stage II crack propagation in the nugget. (c) Fatigue crack initiation and propagation in a JLR bearing specimen, $\Delta\sigma$ = 270 MPa, test interrupted after 50,000 cycles (~ 50% of fatigue lifetime). Average crack propagation indicated with a white arrow; same specimen orientation in (a,b,c)

3.2.2. Fatigue properties of JLR bearing welds

The fatigue strength of JLR bearing specimens is close to that of sound weld specimens. For data points 4 and 5 in Fig. 5, fracture initiated from the TMAZ at the top surface, so that any possible influence of a small flash could not be discarded. The slight difference evidenced from Table 2 and Fig. 5 is much lower than that reported in literature [3, 16-18] for 5083, 2024 and 7075 alloys. However, in the present study only, JLR bearing welds were quantitatively compared with sound welds realized with the *same* base metal and welding conditions. From the two interrupted tests, only one specimen showed indications of fatigue crack initiation and propagation from the bottom surface of the nugget, yet over limited distance (Fig. 6c). This suggests that for the investigated load level, the crack initiation lifetime could be close to 50% of the total fatigue lifetime.

3.2.2. Fatigue properties of KB bearing welds

As the KB is tilted by only about 20° with respect to the loading axis over a depth of about 20 µm (Fig. 1b), two preparation procedures were used for the bottom surface of KB bearing fatigue specimens. The first set of specimens was tested with as-welded bottom surface. The lower surface of the second set of specimens was ground over about 20 µm as for sound and JLR bearing welds. Only in the latter case did the part of KB that was nearly perpendicular to the loading axis intersect the bottom free surface of the specimens.

A significant difference in lifetime was observed between both sets of specimens (Fig. 5). Crack initiation in ground KB bearing specimens occurred at the KB for $\Delta\sigma$ > 255 MPa, i.e., for a maximum stress higher than the value of 280 MPa that was also required to open the KB under uniaxial tension. The fracture surface of the KB (Fig. 7) was similar to that observed after uniaxial tension and to that reported in [8]. After 7,000 (respectively, 15,000) cycles, the fracture surface

evidenced local opening of the KB over 60-80 µm (respectively, ~50 µm) followed by fatigue crack propagation over 30-40 µm (respectively, 30-55 µm) (Fig. 7c). Thus, even after only 20% of the fatigue lifetime, crack initiation and propagation was observed from place to place all along the KB as in [7, 8]. This confirms that at high stresses, early crack initiation occurs due to opening of the KB, most probably during the first cycle. At lower stresses, crack initiation occurred away from the KB but the lifetime was still significantly lower than that of sound or JLR bearing welds (data points 6 to 9 in Fig. 5). In KB specimens with an as-welded lower surface, the crack initiation site (either at the KB, or from surface defects far from the KB) did not significantly depend on the load level. This suggests that the effect of the as-welded KB on the fatigue lifetime could be of the same order as that of surface defects after welding.

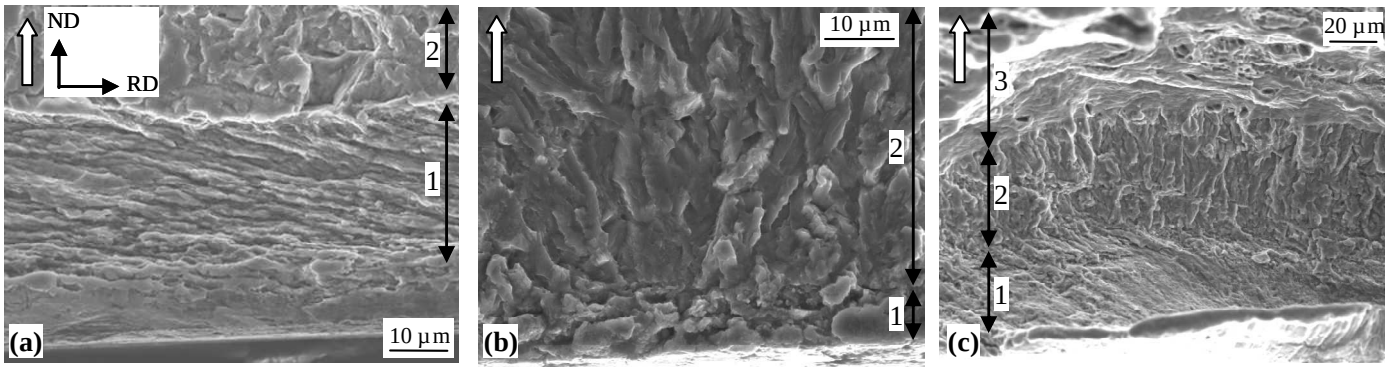

Figure 7. Fracture surface of KB bearing specimens (a) with a ground bottom surface, $\Delta\sigma$ = 306 MPa, lifetime ~13,000 cycles with the crack propagating in mode I along the exposed KB, (b) with an as-welded bottom surface; initiation at, and propagation away from the KB, $\Delta\sigma$ = 279 MPa, lifetime ~70,000 cycles; (c) with a ground bottom surface, $\Delta\sigma$ = 279 MPa, interrupted after 15,000 cycles. (1), (2), and (3) respectively denote cracking along the KB, away from the KB and under uniaxial tension. Average crack propagation indicated with a white arrow; same specimen orientation in (a,b,c)

3.2.3. Fatigue properties of Gap3 and Gap7 bearing welds

The lifetime of Gap bearing welds was significantly lower than that of the other cross-weld specimens (Fig. 5 and Table 2). In all Gap7 specimens and in Gap3 specimens tested at higher stresses, fracture initiated from small regions close to the bottom surface and showing intergranular decohesions (Fig. 8), similar to those found after uniaxial tension (Fig. 4d). This suggests that in these conditions, the Gap-induced defects strongly affect the lifetime at crack initiation. Even when the fatigue crack did not initiate from such regions, the lifetime was low, as already found for KB bearing welds.

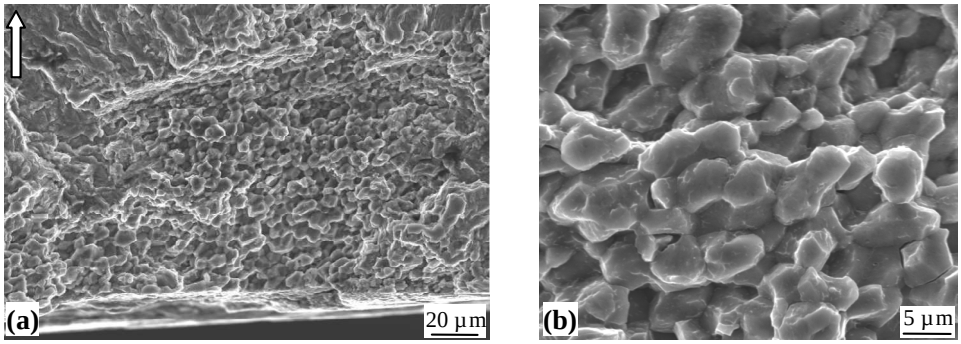

Figure 8. (a) Fatigue crack initiation from “sensitive” GBs of a Gap3 bearing specimen, $\Delta\sigma$ = 256 MPa, lifetime ~26,500 cycles. The average crack propagation is indicated with a white arrow and the specimen orientation is the same as in Fig. 7a. (b) Detailed view of intergranular fracture of “sensitive” GBs

4. Discussion

4.1. Estimation of the crack propagation threshold

To tentatively derive a crack propagation rate from experimental data, ground KB bearing specimens tested at higher stresses were selected because (i) crack initiation was thought to occur during the first cycle, so that the number of cycles corresponding to crack propagation could be easily estimated, and (ii) because crack initiation occurred all along the KB, so that to a first approximation, the crack could be considered to affect the whole width of the specimens. Under these assumptions, a very simple estimate of the stress intensity factor was made by considering a crack of length *a*, propagating in pure Mode I from one side of an infinite plate, leading to the following equation [19]:

$$K_I = \sigma\sqrt{\pi\, a}\; Y\left(\frac{a}{W}\right) = \sigma\sqrt{\pi\, a}\left[1.12 - 0.231\left(\frac{a}{W}\right) + 10.55\left(\frac{a}{W}\right)^2 - 21.72\left(\frac{a}{W}\right)^3 + 30.39\left(\frac{a}{W}\right)^4\right] \quad (2)$$

In Eq. (2), *W* is the length of the ligament, here nearly equal to the plate thickness (3 mm). Eq. (2) was applied to all KB bearing specimens showing crack initiation from the KB, by using the minimum length over which KB opening was observed. This yielded a lower bound value for the stress intensity factor after opening of the KB defect. Fig. 9a shows a threshold for crack propagation in KB bearing welds of about 1 MPa√m, close to that reported for 2198-T8 base metal with the same load ratio (Fig. 9b). As-welded specimens exhibited only slight opening of the (tilted) KB, leading to Mode I stress intensity factors close to the threshold value (data points 1 to 3 in Fig. 5). This could explain why their fatigue lifetime was not correlated with the fracture initiation locus.

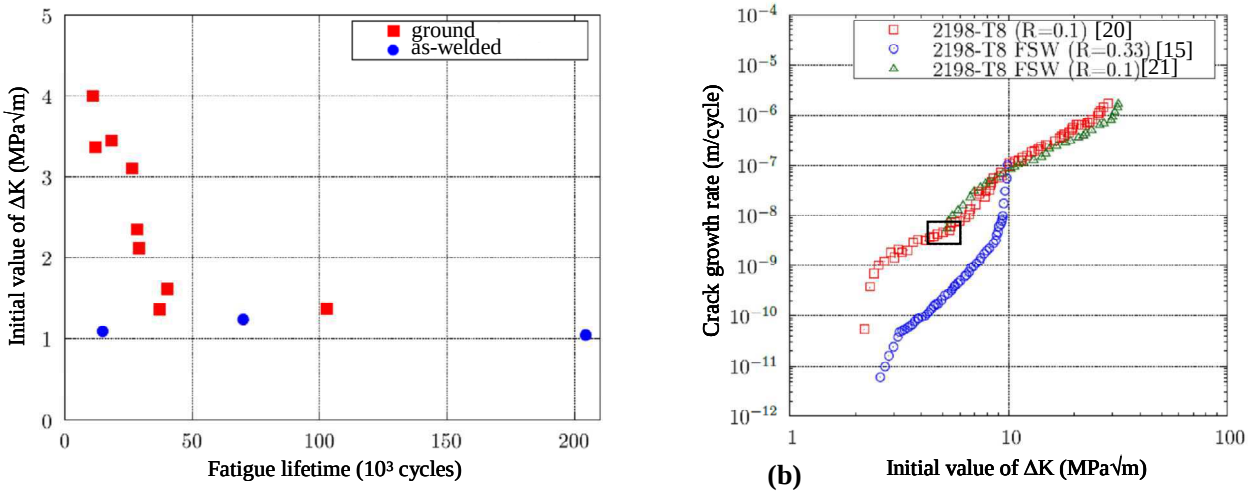

Figure 9. (a) Initial value of ΔK_I for KB bearing welds with either ground or as-welded lower surfaces, showing an apparent threshold value of about 1 MPa√m. (b) Comparison of estimated crack propagation rates during interrupted tests on KB bearing specimens (black box) with literature data

4.2. Estimation of the crack propagation rate in ground KB bearing specimens

To tentatively derive a value of the average crack propagation rate over a small distance, Eq. (2) was used (i) after opening of the KB, and (ii) after interrupted crack propagation. As the length of the fatigue crack varied from place to place, minimum and maximum values were used, leading to upper and lower bounds listed in Table 3. These values are consistent with literature data obtained using the same load ratio (Fig. 9b).

Table 3. Determination of average crack propagation rate from interrupted tests on KB bearing welds

Δσ = 279 MPa, ground bottom surface	After 7,000 cycles (≈ 20% of lifetime)	After 15,000 cycles (≈ 40% of lifetime)
Δ*K* after opening of KB (MPa√m)	4.3	4.3
Δ*K* after fatigue crack propagation (MPa√m)	5.2 - 5.8	5.5 - 6.1
Average value of crack growth (10^{-9} m/cycle)	4.3 - 7.1	2.6 - 4.0

4.3. Effect of welding conditions on fatigue crack initiation and propagation

In KB and Gap bearing specimens, the defect clearly affects crack initiation mechanisms, leading to a strong reduction in fatigue lifetime at high stresses. The fatigue lifetime at low stresses cannot be related to an obvious effect of defects on crack initiation, hardness or tensile strength, while it is significantly affected by the change in welding conditions. Thus, changing the welding conditions not only produced "visible" defects, but also influenced the sensitivity of the welds to fatigue crack initiation even away from those defects. Consequently, the effect of such changes on the fatigue strength cannot be inferred from using only tensile test results and metallographic inspection of the welds. For a maximal stress lower than the yield strength of the nugget (horizontal line in Fig. 5), residual stresses cannot be relieved during the fatigue test and have to be taken into account to further interpret data from e.g. Gap3 and Gap7 bearing specimens. The estimated crack propagation rate in KB bearing specimens seems to be close to that reported in literature (Fig. 9b), indicating that crack propagation could be less affected than crack initiation by the change in welding conditions. More experimental data points are needed to confirm this result.

5. Conclusions

Tension-tension fatigue tests on 2198-T851 butt friction stir welds led to the following conclusions.

- The effect of the joint line remnant is negligible in the investigated conditions.
- The kissing bond opens during tension or during the first fatigue cycle if the maximum stress is higher than about 280 MPa. The crack growth rate (4-7.10^{-9} m/cycle) is consistent with literature data. The threshold stress intensity factor amplitude, Δ*K*, for crack propagation is close to 1 MPa√m.
- A clearance of 10% of the sheet thickness is large enough to trigger local intergranular decohesions close to the lower surface of the nugget, for sufficiently high values of stresses. A clearance of 23% of the sheet thickness systematically leads to premature crack initiation by intergranular decohesions both in uniaxial tension and fatigue tests. The resulting low fatigue strength could be affected by residual stresses because no large scale plastic strain develops in that particular case.
- The change in welding conditions seems to lower the fatigue strength even far away from the visible defects, while keeping hardness and tensile properties almost unaffected. The appearance of defects is not the only consequence of this change that influences fatigue properties.

Acknowledgements
This study was supported by the FNRAE (National Aerospace Foundation) under "MASAE" grant.

References

[1] P. L. Threadgill, A. J. Leonard, H. R. Shercliff, P. J. Withers, Friction stir welding of aluminium alloys. Int. Mater. Rev., 54 (2009) 49-93.

[2] Y. S. Sato, H. Takauchi, S. H. C. Park, H. Kokawa, Characteristics of the kissing-bond in friction stir welded Al alloy 1050. Mater. Sci. Eng., A405 (2005) 333-338.
[3] S. Di, X. Yang, G. Luan, B. Jian, Comparative study on fatigue properties between AA2024-T4 friction stir welds and base materials. Mater. Sci. Eng., A435-436 (2006) 389-395.
[4] H. B. Chen, K. Yan, T. Lin, S. B. Chen, C. Y. Jiang, Y. Zhao, The investigation of typical welding defects for 5456 aluminum alloy friction stir welds. Mater. Sci. Eng., A433 (2006) 64-69.
[5] Y. Uematsu, K. Tokaji, H. Shibata, Y. Tozaki, T. Ohmune, Fatigue behaviour of friction stir welds without neither welding flash nor flaw in several aluminium alloys, Int. J. Fatigue, 31 (2009) 1443-1453.
[6] L. Cui, X. Yang, G. Zhou, X. Xu, Z. Shen, Characteristics of defects and tensile behaviors on friction stir welded AA6061-T4 T-joints. Mater. Sci. Eng., A543 (2012) 58-68.
[7] T. L. Dickerson, J. Przydatek, Fatigue of friction stir welds in aluminium alloys that contain root flaws. Int. J. Fatigue, 25 (2003) 1399-1409.
[8] C. Zhou, X. Yang, G. Luan, Effect of root flaws on the fatigue property of friction stir welds in 2024-T3 aluminum alloys. Mater. Sci. Eng., A418 (2006) 155-160.
[9] J. E. Barnes, J. Mc Michael, A. Reynolds, Effects of friction stir welding defects on 7075 joint strength and fatigue life, in: Proc. 6th Int. Symp. on Friction Stir Welding, Curran Associates, Inc., New York, 2006 (CD-ROM).
[10] B. K. Christner, G. D. Sylva, Friction stir welding development for aerospace application, in: Int. Conf. on Advances in Welding Technology, Joining of High Performance Materials, Columbus, OH, 1996.
[11] T. Le Jolu, T. F. Morgeneyer, A. Denquin, J. Besson, A. F. Gourgues-Lorenzon, Characterisation of internal welding defects and effect on the plastic behaviour of FSW joints of AA2198 Al-Cu-Li alloy, to be submitted to Mater. Sci. Eng. A (2013).
[12] A. Denquin, D. Allehaux, G. Lapasset, H. Ostersehlte, Microstructural phenomena of FSW joints; friction stir welding behaviour of 2098 type alloys and resulting weld properties, in: G. Gottstein, J. Hirsch, B. Skrotzki (Eds.), 11th Int. Conf. on aluminium alloys, Wiley, 2008, pp. 1939-1944.
[13] H. J. Liu, H. Fujii, M. Maeda, and K. Nogi, Tensile properties and fracture locations of friction-stir-welded joints of 2017-T351 aluminum alloy. J. Mater. Proc. Technol., 142 (2006) 692-696.
[14] K. Kumar and S. V. Kailas, Positional dependence of material flow in friction stir welding: analysis of joint line remnant and its relevance to dissimilar metal welding. Sci. Technol. Welding Joining, 15 (2010) 305-311.
[15] P. Cavaliere, A. De Santis, F. Panella, A. Squillace, Effect of anisotropy on fatigue properties of 2198 Al-Li plates joined by friction stir welding. Eng. Failure Analysis, 16, (2009) 1856-1865.
[16] C. Z. Zhou, X. Q. Yang, G. H. Luan, Effect of kissing bond on fatigue behavior of friction stir welds on Al 5083 alloy. J. Mater. Sci., 41 (2006) 2771-2777.
[17] C.Z. Zhou, X. Q. Yang, G. H. Luan, Effect of oxide array on the fatigue property of friction stir welds. Scr. Mater., 54 (2006) 1515-1520.
[18] S. Di, X. Yang, D. Fang, G. Luan, The influence of zigzag-curve defect on the fatigue properties of friction stir welds in 7075-T6 Al alloy. Mater. Chem. Phys., 104 (2007) 244-248.
[19] H. Tada, P. C. Paris, G. R. Irwin, The stress analysis of cracks handbook. Del Research Corp. Saint Louis, 1973.
[20] S. Richard, Fatigue cracking of third generation aluminium-lithium alloys, PhD dissertation, http://tel.archives-ouvertes.fr/docs/00/60/54/26/PDF/ThA_se_SA_bastien_RICHARD_2011.pdf, ENSMA, Poitiers, France (in French).
[21] Y. E. Ma, P. E. Irving, T. Fisher, X. Zhang, G. Servetti, Effects of residual stresses on fatigue crack propagation in friction stir welded 2198-T8 and 2195-T8 Al-Li alloy joints, in: 12th International Conference on Fracture, Curran Associates, Inc., New York 2010, 1797-1806.